ELSEVIER

Marine Geology 219 (2005) 155–171

MARINE GEOLOGY
INTERNATIONAL JOURNAL OF MARINE GEOLOGY, GEOCHEMISTRY AND GEOPHYSICS

www.elsevier.com/locate/margeo

Neotectonic structures in İzmir Gulf and surrounding regions (western Turkey): Evidences of strike-slip faulting with compression in the Aegean extensional regime

Neslihan Ocakoğlu [a,*], Emin Demirbağ [a], İsmail Kuşçu [b]

[a] *İstanbul Teknik Üniversitesi, Maden Fakültesi, Jeofizik Mühendisliği Bölümü, Maslak 80626, İstanbul, Turkey*
[b] *Maden Tetkik ve Arama Genel Müdürlüğü, Jeoloji Dairesi, Eskişehir Yolu, 06520 Ankara, Turkey*

Received 11 September 2003; received in revised form 6 June 2005; accepted 16 June 2005

Abstract

Of single channel, 70 km, and 900 km of multi-channel seismic reflection data show that İzmir Gulf and surrounding regions are widely deformed by N–S to NE–SW trending active transpressional strike-slip faults, reverse faults and some E–W normal faults. Normal faults are mapped offshore Karaburun–Foça, in inner part of İzmir Gulf; offshore Alaçatı–Teke and offshore Kuşadası delimiting the southern scarp of Lesvos basin, İzmir basin, northern scarp of Ikaria basin and continuation of Küçük Menderes Graben, respectively. Normal faults are cut by strike-slip faults. The major strike-slip faults are the N–S oriented Karaburun reverse fault bordering İzmir Gulf on the west and uplifting the Karaburun Peninsula and the NE–SW oriented strike-slip Tuzla Fault extending from Doğanbey Promontory towards Seferihisar ridge onland. This fault pattern can be explained by pure-shear model indicating that the area is under E–W compression, N–S extension, NE–SW and NW–SE strike-slip deformation. Moreover, Tuzla Fault has a regional importance. It separates NE–SW trending structures of the study area from E–W oriented Gediz and Küçük Menderes grabens and probably continues towards to İznik at north constituting a transition zone between northern transpressional region and southern extensional region in the western Anatolia–Aegean Sea.

Keywords: Aegean sea; western Anatolia; İzmir Gulf; strike-slip faulting; reverse faulting; seismic reflection

1. Introduction

The study area is located in the central Aegean Sea, along the western coast of Anatolia including İzmir Gulf and areas offshore from Alaçatı, Doğanbey and Kuşadası (Fig. 1). Western Anatolia and Aegean Sea are commonly considered as under N–S extension in

* Corresponding author. Fax: +90 212 285 6201.
E-mail addresses: neslihan@itu.edu.tr (N. Ocakoğlu), demirbag@itu.edu.tr (E. Demirbağ), environ@mtabim.mta.gov.tr (İ. Kuşçu).

0025-3227/$ - see front matter © 2005 Elsevier B.V. All rights reserved.
doi:10.1016/j.margeo.2005.06.004

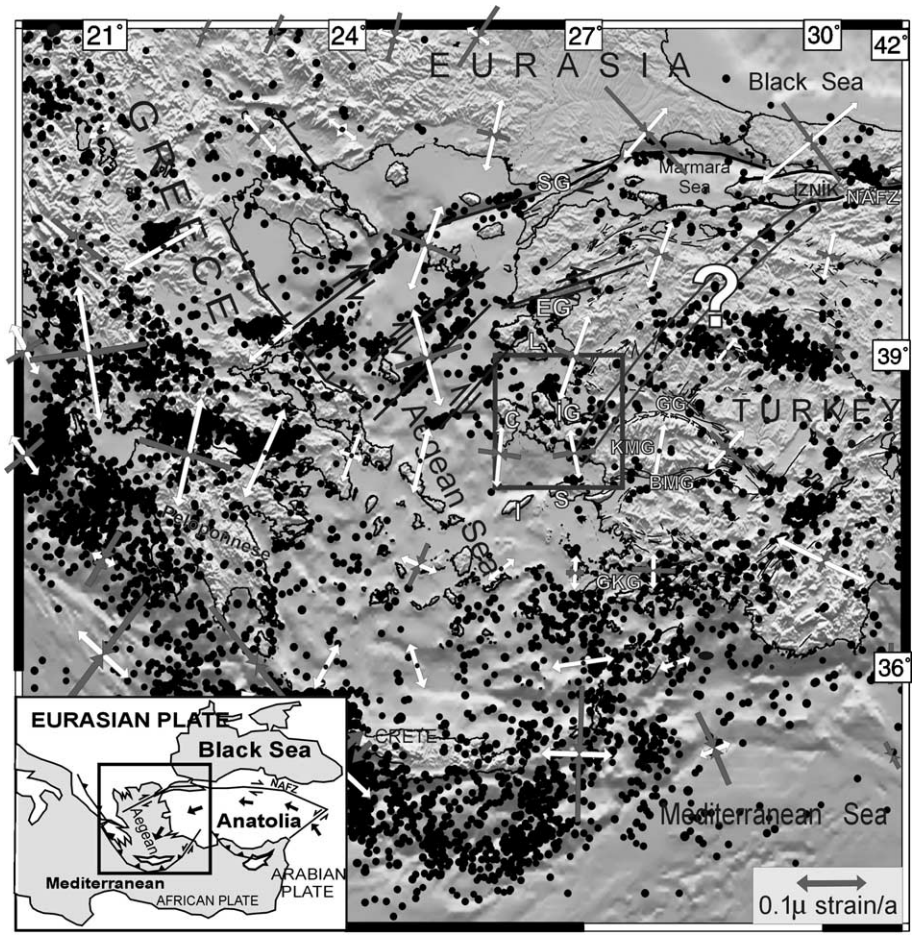

Fig. 1. Simplified faults, instantaneous deformation, seismicity, topography and bathymetry map of the Aegean region. Instantaneous deformation with white and gray arrows show extension and compression strain rates, respectively calculated from the velocity field in the eastern Mediterranean relative to a Europe-fixed reference frame by GPS data (modified from Kahle et al., 1998). Note N–S oriented extensional and E–W oriented compression strain rates in the study area. Seismicity with International Seismological Center (ISC) epicentres for $M_w \geq 4$ earthquakes between 1964–1997 are also shown. There is a seismically active zone for $4 \leq M_w \leq 5$ earthquakes along a NE trend between the study area and İznik. Abbrevations are: NAFZ—North Anatolian Fault Zone, SG—Saros Gulf, EG—Edremit Gulf, L—Lesvos island, İG—İzmir Gulf, C—Chios island, S—Samos island, I—Ikaria island, GG—Gediz Graben, KMG—Küçük Menderes Graben, BMG—Büyük Menderes Graben, GKG—Gökova Graben. Inset shows regional framework: arrows indicate sense of motion relative to the Eurasian plate.

response to westward motion of Anatolian block which is in collision with Arabian Plate (McKenzie, 1972; Dewey and Şengör, 1979) (Fig. 1 inset). However, the topographic and bathymetric features and instantaneous deformation of Aegean region based on seismicity and strain rates from GPS data indicate complexity of structures from north to south and raise some questions about active tectonism of the Aegean region, as to whether whole region is under a pure N–S extension regime or not (Fig. 1). Mascle and Martin (1990) divided the Aegean region into three main areas. The northern Aegean area is well known to be developed under the influence of the North Anatolian Fault Zone (NAFZ). When NAFZ enters into the north Aegean sea, it splits into branches bending south, in Saros and Edremit gulfs and the north Aegean trough (Barka and Kadinsky-Cade, 1988; Taymaz et al., 1991; Barka, 1992; Kurt et al., 1999). Bending of branches is shown by GPS strain rates (Kahle et al., 1998) which change from

NNE–SSW extension and ESE–WNW compression to NNW–SSE extension and ENE–WSW compression. The sense of E–W compression along with N–S extension in this area can be explained by continental collision occurring at NW Greece, which resists to the westward motion of northern Aegean. Güney et al. (2001) show that a positive flower structure of a strike-slip fault cuts the normal fault in Edremit Gulf.

On the other hand, the southern Aegean area, which is morphologically characterized by separate troughs (Mascle and Martin, 1990), is under the influence of Hellenic subduction and Pliny–Strabo Fault Zone (Le Pichon and Angelier, 1979; Woodside et al., 2000; Huguen et al., 2001; Piper and Perissoratis, 2003). The sinistral Fethiye–Burdur Fault Zone was interpreted as the onshore extension of Pliny–Strabo Fault Zone (Barka and Reilinger, 1997). The offshore area of Crete Island was interpreted as an extensional area with some NE–SW directed dextral strike-slip faults (Piper and Perissoratis, 2003). The GPS strain rates show mostly pure N–S extension in this area. The rapid SW motion of southwestern Anatolia and southern Greece towards the Hellenic arc with values of 30 ± 2 mm/year (McClusky et al., 2000) can be explained by a lack of collision in SW Greece, whereas NW Greece is blocking the westward motion of Anatolia.

Under these geodynamic settings in the Aegean, the study area seems to be a puzzle both from its morphological and structural point of view. İzmir Gulf (İG) incompatibly extends in a NNW–SSE direction across E–W grabens of western Anatolia, such as Gediz Graben (GG), Küçük Menderes Graben (KMG) and Büyük Menderes Graben (BMG) (Fig. 1). Both active normal and strike-slip faulting are observed in the area. Kaya (1979, 1981) determined İzmir Gulf as a Neogene depression, which is formed by N–NE trending blocks, by steep, oblique faults and smaller E–W striking normal faults between these N–NE trends cutting them. He partly noticed that these Neogene structures influenced Quaternary tectonics in the area. According to some researchers (Şengör et al., 1984; 1985; Seyitoğlu and Scott, 1994; Yılmaz et al., 2000), these N–NE trending faults accommodate on hanging walls of E–W grabens and do not offset the footwall of grabens. Although NW–SE extension of İzmir Gulf and N–S to NE–SW structures of the surrounding area are seen as dominant trends across the E–W grabens, these authors considered them as secondary features in the area. Moreover, there are some other onland studies that show active N–S to NE–SW trending faults with strike-slip character in the study area (Şaroğlu et al., 1992; Emre and Barka, 2000; Altunkaynak and Yılmaz, 2000; Genç et al., 2001). In addition, offshore Samos island, Lykousis et al. (1995) showed that both northern and southern Ikaria basins were developed under a compressional phase related to transpressional activity during Quaternary. This strike-slip deformation is still active along the southeastern part of the North Ikarian Basin. Also, GPS strain rates show E–W compression as much as N–S extension in this area (Fig. 1). In addition, Stiros et al. (2000) indicated some uplifts on the NW coast of Samos Island and the SE coast of the neighbouring island, Ikaria. They argued that this uplift may be related to either tilting of a normal fault or a strike-slip fault passing through between Samos and Ikaria islands.

These discussions show the necessity of detailed investigation of active structural features of the study area both offshore and onland. Moreover, the seismicity reveals a second importance of the study area in the western Anatolia in terms of regional setting. Fig. 1 shows that a seismicity zone ($4 \leq M_w \leq 5$) extends between the study area and İznik, bordering the E–W grabens of Anatolia and with a dense E–W trending seismicity to the north of grabens. Crampin and Evans (1986) suggested that this seismic activity can identify an active boundary. From this point of view, they defined the Marmara block behaving as a separate tectonic unit with its eastern boundary bordered by this NE–SW seismicity zone.

Considering the discussions above, we acquired approximately 900 km of multi-channel and 70 km of single-channel seismic reflection data and we processed and interpreted them to address the following questions:

1. What are the main structural and stratigraphic features of the İzmir area?
2. Are the structural features of the İzmir area and adjacent land areas similar or not?
3. Can the structural features of the study area constitute a transition zone between the northern and southern Aegean regions?

2. Geological, seismological and geomorphological setting

Onshore geology map shows that the study area is widely covered by Mio–Pliocene and younger units (Fig. 2). Additionally, Pre-Miocene basement, which consists of Silurian, Carboniferous, Triassic, and Cretaceous rocks, only crops out along high elevated areas such as Karaburun, Seferihisar, and Kuşadası ridges (Fig. 2). In the study area, several faults are seen, some of which are determined to be active faults (marked with bold lines on Fig. 2) and the others are undetermined and reverse faults are related to paleo-tectonic activities (thin lines on Fig. 2). Even though these faults are mapped as inactive, they align with lineaments on the morphology which will be discussed in the following paragraphs (compare Figs. 2 and 3B). The previous onland studies give more knowledge about the active faults of the study area than the geology map. These faults marked on morphology (Fig. 3B) are called as Karaburun Fault (KF), Urla Fault (UF), Bornova Fault (BF), İzmir Fault (İF) and Küçükmenderes Fault (KMF) (Erinç, 1955; Dumont et al., 1979; Dewey and Şengör, 1979; Kaya, 1979; Şaroğlu et al., 1992; Emre and Barka,

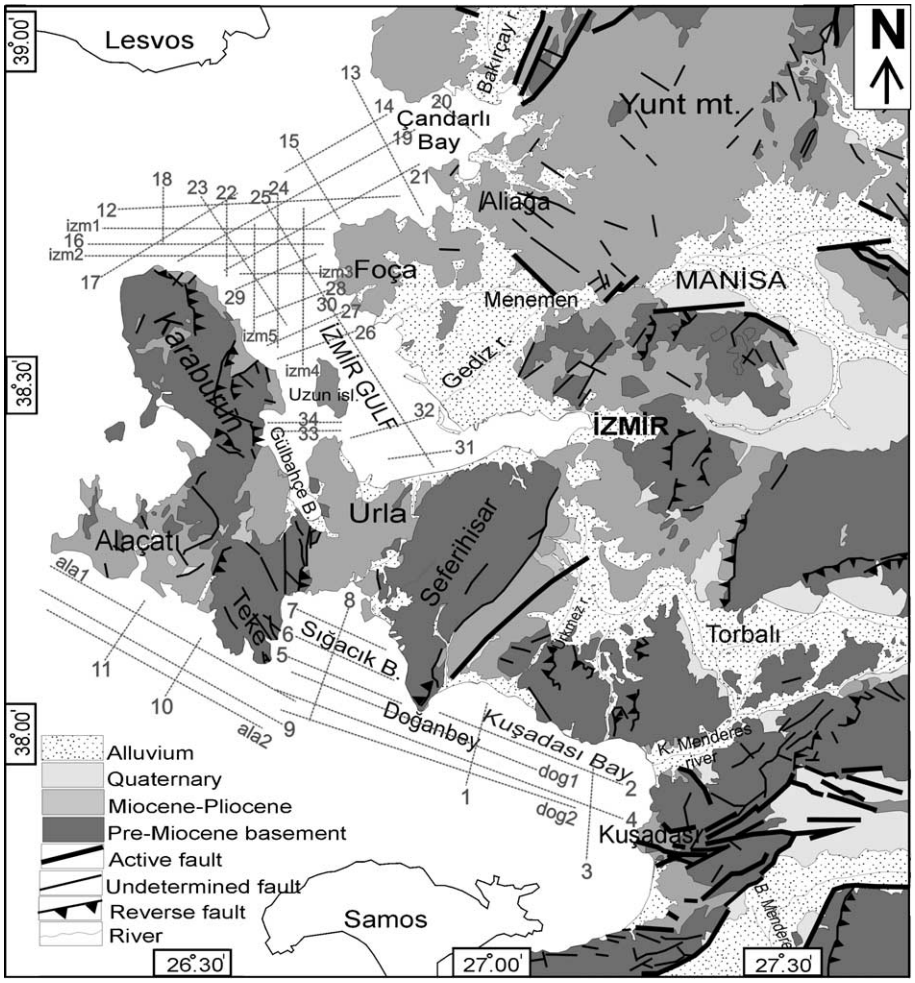

Fig. 2. Geology map of the study area (simplified from MTA 1 : 500,000 scale geology map) and location of the seismic lines. Active faults are marked onland with bold lines.

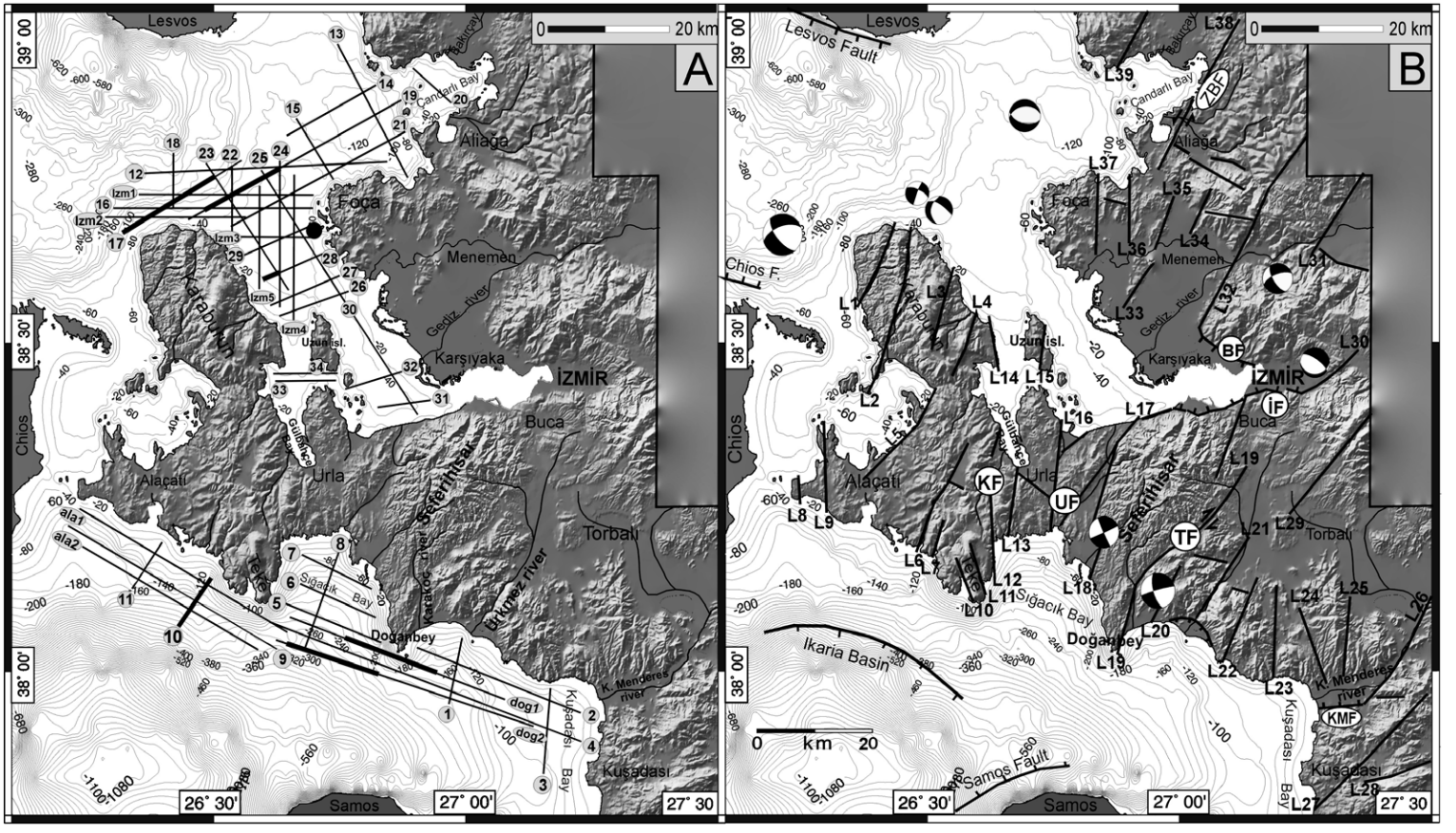

Fig. 3. (A) Map of the study area showing detailed topography obtained by digitising 20 m contours of 1:25,000 scale topographic maps of the Turkish General Command of Mapping with ~75 m precision and bathymetry taken from the Turkish Navy with ~350 m precision and location of the seismic lines. Highlighted segments of these lines are displayed in article. Location of Foça-1 well (TPAO, 1987) is shown by bold circle. (B) Active onland faults; ZBF—Zeytindağ–Bergama Fault, BF—Bornova Fault, İF—İzmir Fault, KF—Karaburun Fault, UF—Urla Fault, TF—Tuzla Fault, KMF—Küçük Menderes Fault (Kaya, 1979; Şaroğlu et al., 1992; Emre and Barka, 2000; Genç et al., 2001), offshore faults (Mascle and Martin, 1990) and the main lineaments (L) are shown with black lines. Fault plane solutions for recent earthquakes from McKenzie (1972), Kocaefe and Ataman (1976), Drakopoulos and Delibasis (1982), Kalafat (1995), Tan and Taymaz (2001, 2003) are also added on figure.

2000; Altunkaynak and Yılmaz, 2000; Genç et al., 2001). In spite of these onland studies, there are a few offshore study showing active faults. Mascle and Martin (1990) mapped some E–W trending normal faults bordering the main offshore basins. They called them as Lesvos Fault, Chios Fault, Samos Fault and Ikaria Fault (Fig. 3B). These E–W faults are compatible with onland normal faults (BF, İF and KMF) with their orientations and characters (Fig. 3B).

In this study, linear scarps, long valleys and displaced shore lines are considered as constituting a lineament. The lineament map in Fig. 3B show that N–S to NE–SW oriented lineaments are more common on morphology than E–W ones. Some of NE–SW trending lineaments correspond to strike-slip faults. The important ones are Zeytindağ–Bergama left lateral fault zone extending to SW coast of Çandarlı Bay (Şaroğlu et al., 1992) and Tuzla Fault extending at NE–SW along 40 km between İzmir and Kuşadası (Emre and Barka, 2000; Genç et al., 2001). These faults can be traceable on morphology with lineaments L38, L39 and L19, respectively. Especially, the character of Tuzla fault (L19) is well recognised by recent earthquakes (M_w 6.0; Tan and Taymaz, 2001) that occurred on Doğanbey promontory. Although left-lateral slip is seen on morphology at Doğanbey promontory, the focal mechanism solutions show right-lateral slip on Tuzla fault (Tan and Taymaz, 2001). In addition, Emre and Barka (2000) measured ~200–700 m of right lateral slip from the offset of river channels. Therefore, we considered that Tuzla fault is right-lateral strike-slip fault. The other focal mechanism solutions of recent earthquakes in the study area indicate both normal faulting and strike-slip faulting (Fig. 3).

The other lineaments marked on the morphology can be described as follows: On Karaburun Peninsula, NE–SW lineaments L1 to L7 delimit the ridges and partly the west coast of the peninsula, some of which may be correlated to the reverse faults in the geology map (compare Figs. 2 and 3B). L8 and L9 extend in N–S direction in Alaçatı. Lineaments L10 and L11 in NNW–SSE bound the Teke peninsula. N–S oriented lineaments L12 to L16 are a surface expression of Karaburun and Urla faults, which may be correlated to reverse and undetermined faults in Urla. These lineaments seem to control the shoreline of Uzun Island and Urla ridge. Uzun Island is affected by a right lateral displacement along L15. Lineaments L20 to L28 south of İzmir more or less extend N–S and NE–SW and shape the morphology around Kuşadası. Lineaments L29 to L33 delimit the Gediz river and the ridges around Torbalı and İzmir city, some of which may be correlated to reverse faults on the geology map (Fig. 2). Finally, lineaments L34 to L37 bound Menemen and Foça ridges.

3. Seismic data acquisition and processing

During two surveys on board MTA Sismik-1 research vessel, approximately 900 km of multichannel and 70 km of single channel seismic reflection profiles were acquired in 1996 and 2000 (Figs. 2 and 3A). Different recording parameters were used in these surveys (Table 1). The data collected in 2000 has shallower penetration and higher resolution, enabling it to have better image sedimentary packages and Miocene basement, whereas the data from 1996 has better penetration but lower resolution.

The seismic data were processed in the Department of Geophysics, at İstanbul Technical University (İTÜ). A conventional data processing stream was applied to the data as follows: data transcription, in-line geometry definition, source–receiver array datum correction, editing, muting of direct

Table 1
Shooting and recording parameters

Parameter	1996 (MC)	2000 (MC)	2000 (SC)
Channels	108	48 or 60	6
Source	9 GI gun	6 GI gun	2 GI gun
Volume (in.^{3})	1080	780	180
Pressure (PSI)	1600	1500	1500
Streamer length (m)	1350	600 or 750	75
Near offset (m)	237.5	50 or 100	30
Far offset (m)	1575	900	105
Shot interval (m)	50	25	10
Group interval (m)	12.5	12.5	12.5
Sampling (ms)	2	2	1
Folding	14	12 or 15	–

GI: Generator–injector airgun, MC: Multi channel, SC: Single channel.

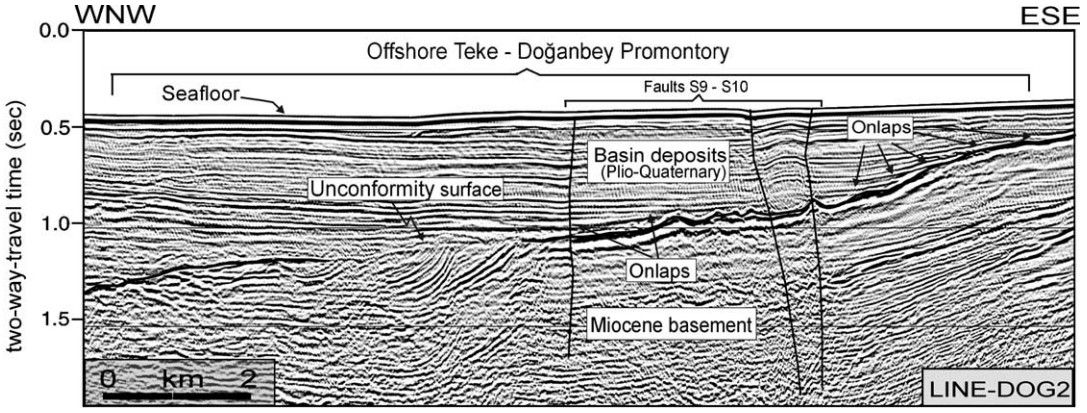

Fig. 4. The seismic section extracted from western part of the line Dog-2 (see Fig. 3A for location). Note that the unconformity surface is well marked by truncated basement reflections at ~1 s. Vertical exaggeration is ~2.

and refracted waves, gain analysis, common depth-point sorting, stacking velocity analysis, normal move-out correction and muting, stacking, spiking and predictive deconvolution, bandpass filtering, finite-difference time migration and automatic gain control. Strong multiple reflections due to the shallow seafloor and basement reflector were observed in the seismic data. These multiples were eliminated as much as possible by predictive deconvolution techniques.

4. Stratigraphic and structural interpretations of the seismic sections

Two main stratigraphic units can be seen on the seismic sections (Figs. 4, 6–10). The lower unit, which has more or less parallel or wavy reflectors, is interpreted as basement whose top is identified by high amplitude reflections indicating an unconformity (Fig. 4, Line-Dog2). The upper seismic sequence is interpreted as basin deposits that onlap the basement surface (Fig. 4). It generally consists of parallel reflectors with good continuity, but frequently cut by faults (Figs. 4, 6–10). Top of the basement unit on line-25 is well correlated with the unconformity between Upper Miocene and Pliocene sediments noted by the Turkish Petroleum Corporation (TPAO) (Foça-1 well, TPAO 1987, Fig. 3A). Also, Yılmaz et al. (2000) and Genç et al. (2001) noted an unconformity between Upper Miocene and Pliocene sediments in western Anatolia. Therefore, the lower and the upper units can be interpreted as the submarine extension of Miocene and older rocks, and Pliocene–Quaternary deposits, respectively.

Contour maps of the basement surface and the thickness of Pliocene–Quaternary deposits were constructed from seismic sections. These maps, in Fig. 5, indicate two main basins on offshore. One of them is located offshore Karaburun, Foça and Lesvos Island in the north, and the other one is located offshore Alaçatı, Doğanbey and Kuşadası in the south. Moreover, two sub-basins are observed in İzmir Gulf. The inner sub-basin (Sb1) deepens to 1000 ms, filled with 900 ms thick basin deposits, which were probably supplied by the Gediz river. The outer one (Sb2) deepens towards the north and connects to the northern main basin. These two sub-basins are separated by a N–S oriented ridge lying between Urla and Foça. This ridge extends onshore along Urla Promontory and Uzun island. Moreover, there is another ridge offshore Doğanbey to the south. This ridge extends onshore along Seferihisar at NE–SW direction.

The basins in Fig. 5 are characterised by active normal faults in the study area. The normal faults were distinguished by smooth vertical discontinuities and vertical displacements on the seafloor and deeper reflection units of seismic sections. They deform both Pliocene–Quaternary deposits and Miocene basement units and generally extend in E–W orientations compatible with contours of the

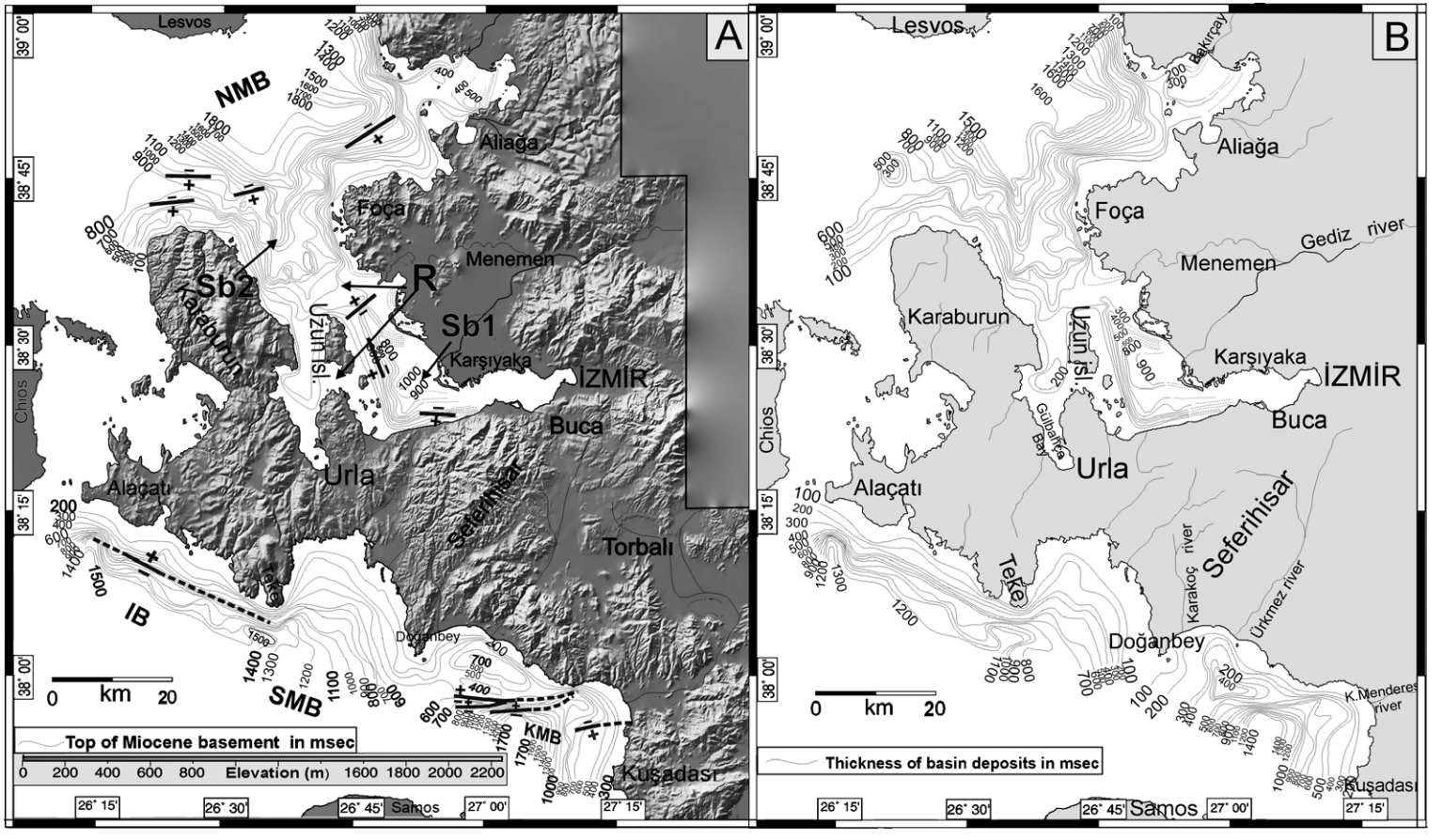

Fig. 5. (A) Shaded topographic image and top of Miocene basement contour map (depths in milliseconds). Gray lines and dashed gray lines show active normal faults and their possible extensions, with footwalls indicated by plus symbol. Abbrevations are: Sb1—Inner sub-basin, Sb2—Outer sub-basin, R—Ridge, NMB—Northern Main Basin, SMB—Southern Main Basin, IB—Ikaria Basin, KMB—Küçük Menderes Basin. (B) Contour map of the thickness of basin sediments in milliseconds.

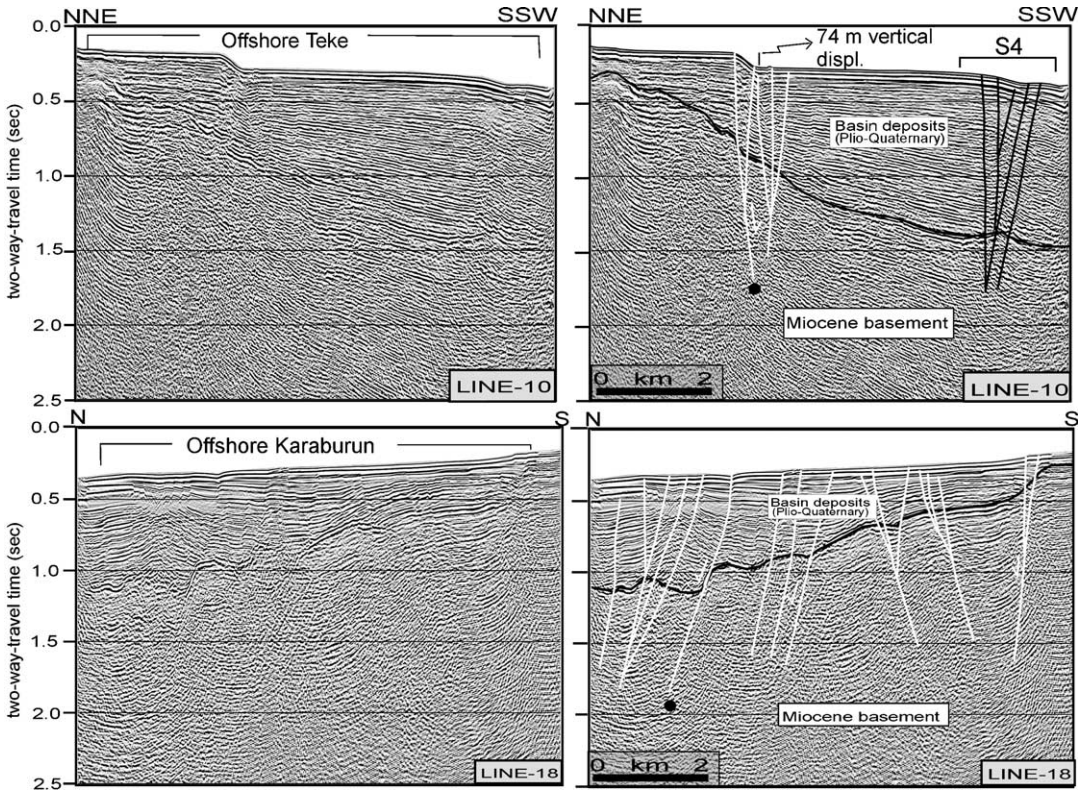

Fig. 6. Time migrated seismic sections, offshore Teke and Karaburun, showing active normal faults marked with white lines and strike-slip faults with black lines (see Fig. 3A for locations). Vertical exaggeration is ~2. Observed vertical displacement on the seafloor and basement surface by normal fault (marked with bold circle on Line-10) looks the same, thus this normal fault is Quaternary age. On line-18, vertical displacement seen on basement units are greater than displacement on Pliocene–Quaternary deposits due to fault marked with a bold circle thus this normal fault can be interpreted as Later Miocene–Pliocene age.

basement surface and thickness of basin deposits (Fig. 5). On Fig. 5A, some normal E–W trending faults border Küçük Menderes basin (KMB) offshore Kuşadası, another NW–SE oriented fault borders the northern scarp of Ikaria Basin (IB). This fault marked on line-10 show the highest vertical displacement with ~74 m in the study area (Fig. 6). Another group of active normal faults borders the north main basin offshore Karaburun (Line-18, Fig. 6). Vertical displacement observed in the seafloor and top of basement by a normal fault which is marked with bold circle in line-10 looks the same. Thus this fault can be interpreted as Pliocene to Quaternary in age. On the other hand, another normal fault on line-18 (marked with bold circle, Fig. 6) shows different vertical displacement at seafloor and the basement surface. Thus this fault should be of late Miocene to Pliocene age.

The N–S and NE–SW trending ridges that are observed on Fig. 5A are recognised on seismic sections by an another group of faults which have generally strike-slip and reverse fault characters (Figs. 7–10). These active strike-slip faults are marked on sections with vertical discontinuities that generally cut the all seismic units and do reach the seafloor or just below it and cause no or minor vertical displacements on the seafloor. Most of them are interpreted as positive flower structures (Figs. 7–10).

N–S to NE–SW trending strike-slip faults are recognised on seismic sections and are well correlated to onland active faults and lineaments (Fig. 11). In the

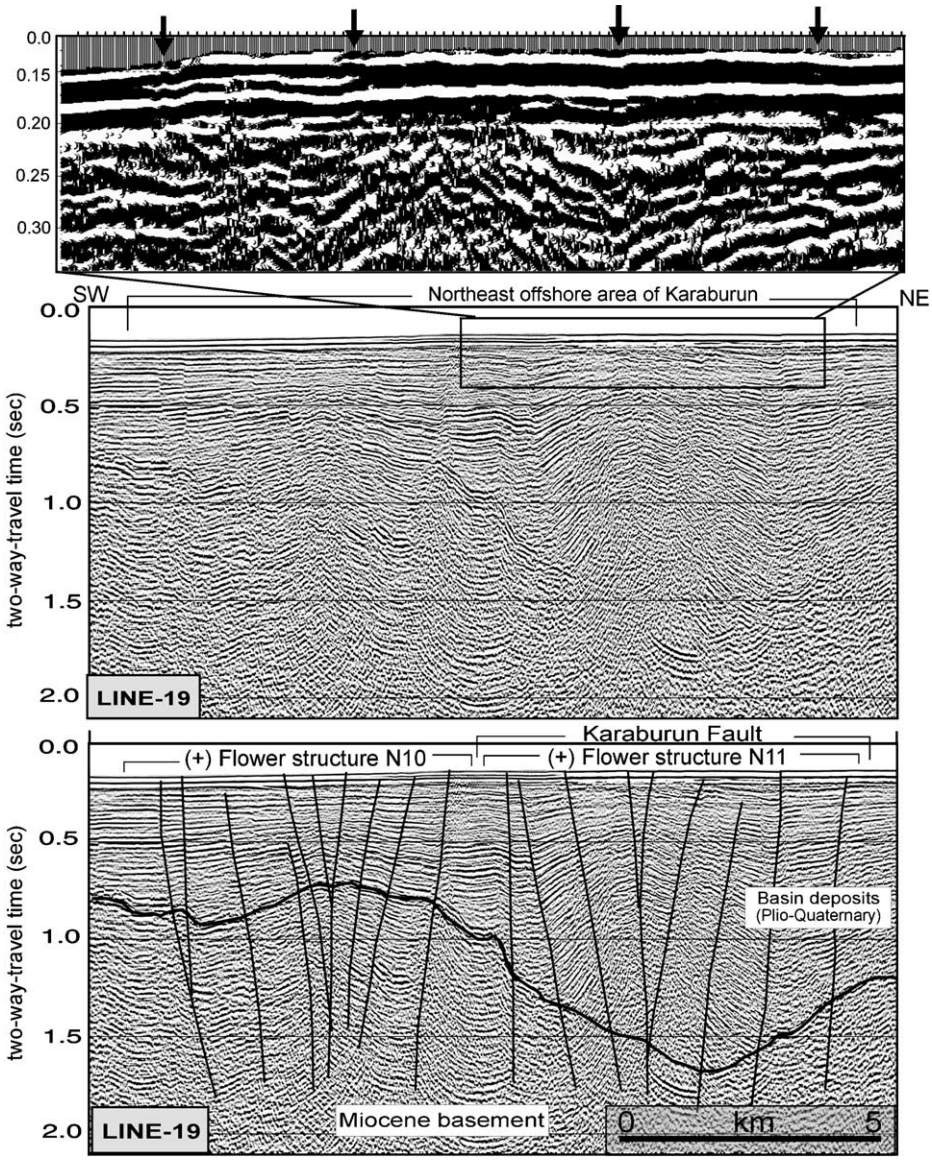

Fig. 7. The western part of line-19 in the entrance of İzmir Gulf shows two active positive flower structures. These strike-slip faults deformed the Miocene basement and Plio–Quaternary sediments. Vertical exaggeration is ~2.5. On the top figure, the black arrows indicate the active faults cutting the seafloor.

entrance of İzmir Gulf, two active positive flower structures cutting Miocene basement and Plio–Quaternary deposits are marked on the western part of line-19 (Fig. 7). As seen in Fig. 7, the top of Miocene basement forms a basin which trends approximately N–S at eastern offshore Karaburun (Sb2 in Fig. 5). It is seen that this basin is highly deformed by a positive flower structure (N11 fault, Fig. 7). N10 and N11 faults gain reverse character along the margins of sub-basin (Sb2) where their orientations turn from NNW–SSE to N–S direction (Compare Fig. 5A with Fig. 11). These faults are correlate well with onland morphology and geology (Compare Fig. 2 to Fig. 11). Especially, N11 fault corresponds to

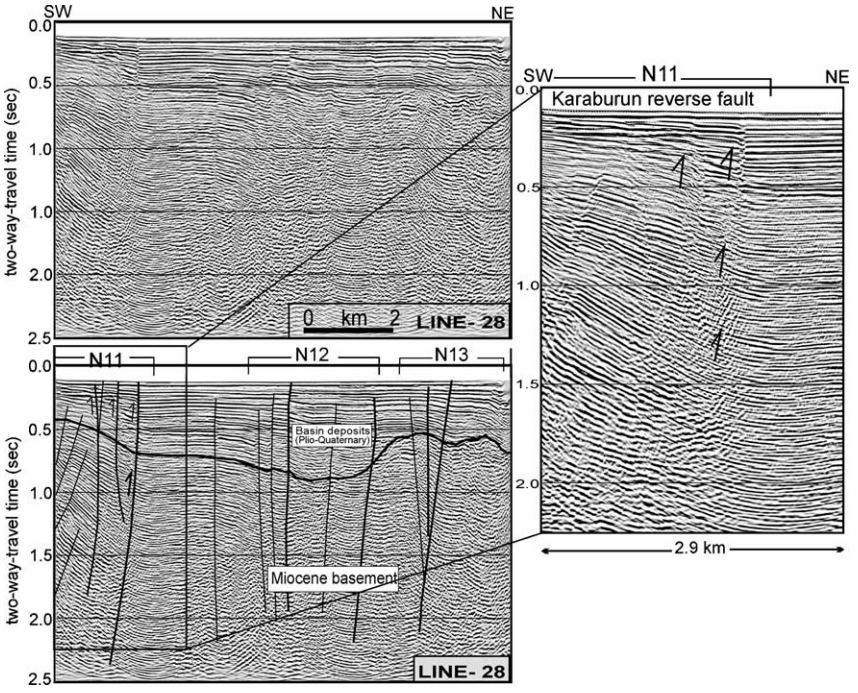

Fig. 8. Line-28 in the eastern side of Karaburun Peninsula. This section shows active Karaburun reverse fault (N11, see details in zoomed section on the right) and the other active strike-slip faults in İzmir Gulf (N12, N13). Vertical exaggeration is ~2.5.

Karaburun Fault (KF) onland (Kaya, 1979; Emre and Barka, 2000) (Fig. 3B). Line-28 in Fig. 8 show that Karaburun fault is an active reverse fault with upthrown reflection levels along all seismic units and raises the Karaburun Peninsula from its eastern edge. The N–S trend of this reverse fault (Fig. 11) is followed from the entrance of the gulf to the southern inner part, Gülbahçe Bay on seismic lines 26 to 29 and 33 and 34. In addition, the faults between N1 to N8 offshore Karaburun (Fig. 11) are marked on seismic line-17 (Fig. 9) as active reverse faults extending in N–S (correlate Figs. 2 and 11). Onshore extension of these faults correlate with the lineaments and reverse faults on the geology map (Fig. 2). Although some of these faults are shown on the onshore geology map (Fig. 2) as passive faults, the zoomed part of Line-17 (Fig. 9) indicates that these faults are active.

The most important active strike-slip fault zone in the study is the Tuzla Fault Zone (S10 and S12), which lies at Doğanbey Promontory (Fig. 10). In Fig. 10, section Dog-1 shows a large active positive flower structure raising Seferihisar Miocene basement units and also deforming Pliocene–Quaternary sediments. S10 and S12 fault zones on seismic section are well correlated with the onshore extension of the Tuzla Fault (Fig. 11). The asymmetry of the Tuzla Fault Zone in cross section (Fig. 10) indicates that this fault is an oblique fault, and thus the eastern faults in this zone should have also reverse component (Fig. 10). This result is also well correlated with onland geology (Fig. 2). Seismic line Dog-1 shows that the Seferihisar horst thrust from west to east at Doğanbey Promontory (correlate Figs. 2 and 10), as seen in the Karaburun reverse fault (Fig. 8). Another important strike-slip fault extends in a N–S direction (S8 fault in Fig. 11) and is connected to the onshore Urla Fault (Kaya, 1979; Genç et al., 2001). This fault borders Gülbahçe Bay at eastern side, and Uzun island at western side and continues towards the north in the gulf with N12 and N13 faults. Other strike-slip faults in the study area can be summarized as follow: faults between S1 to S7 with positive flower character extends onshore at Alaçatı and Teke. N–S trending

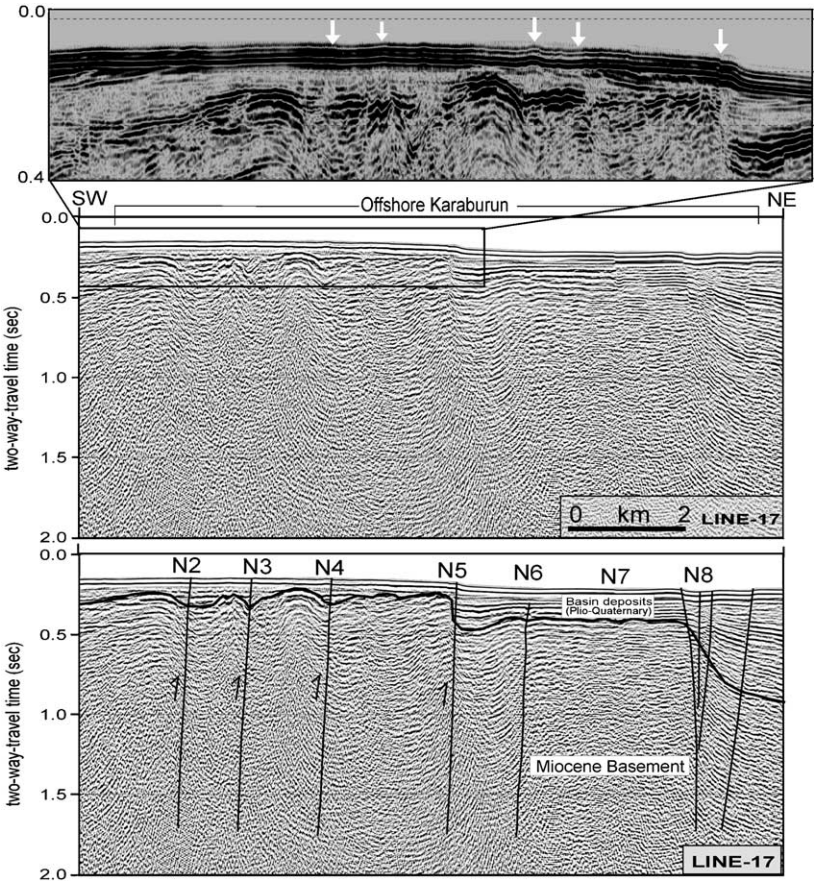

Fig. 9. The western part of seismic Line-17 located offshore Karaburun. The interpreted active reverse faults on this section (see details in zoomed part) are well correlated with onland structures. Vertical exaggeration is ~2.5.

S15 to S18 faults constitute a large positive flower character and cut the E–W trending normal faults of Küçük Menderes Basin offshore Kuşadası. The same style is seen in the E–W trending inner part of İzmir Gulf. NE directed branches of Urla fault cut Sb1 (Fig. 5A) offshore Gediz Delta and are possibly connected with the faults of Foça, Aliağa and Menemen. N15, N16 strike-slip faults (Fig. 11) are correlatable with the NE trending Zeytindağ–Bergama Fault Zone (ZBF) onland (Fig. 11).

5. Discussion and conclusions

The study area is characterized by N–S to NE–SW strike-slip faults, N–S reverse faults and some E–W normal faults (Fig. 11A). These faults generally cut both Miocene basement units and Plio–Quaternary basin deposits.

Normal faults marking the inner part of İzmir Gulf and offshore Kuşadası are well correlated with the E–W oriented İzmir Fault (İF) and Küçük Menderes Fault (KMF), respectively (Fig. 11A). The other E–W normal faults are located at the northern scarp of Ikaria basin offshore Alaçatı–Teke and at the southern boundary of the north main basin offshore Karaburun. The normal faults are disturbed frequently by strike-slip faults (Fig. 11A). The strike-slip faults are interpreted as primary active faults both offshore and onshore (Fig. 11A). These faults generally have transpressional character such as NE–SW trending Tuzla fault

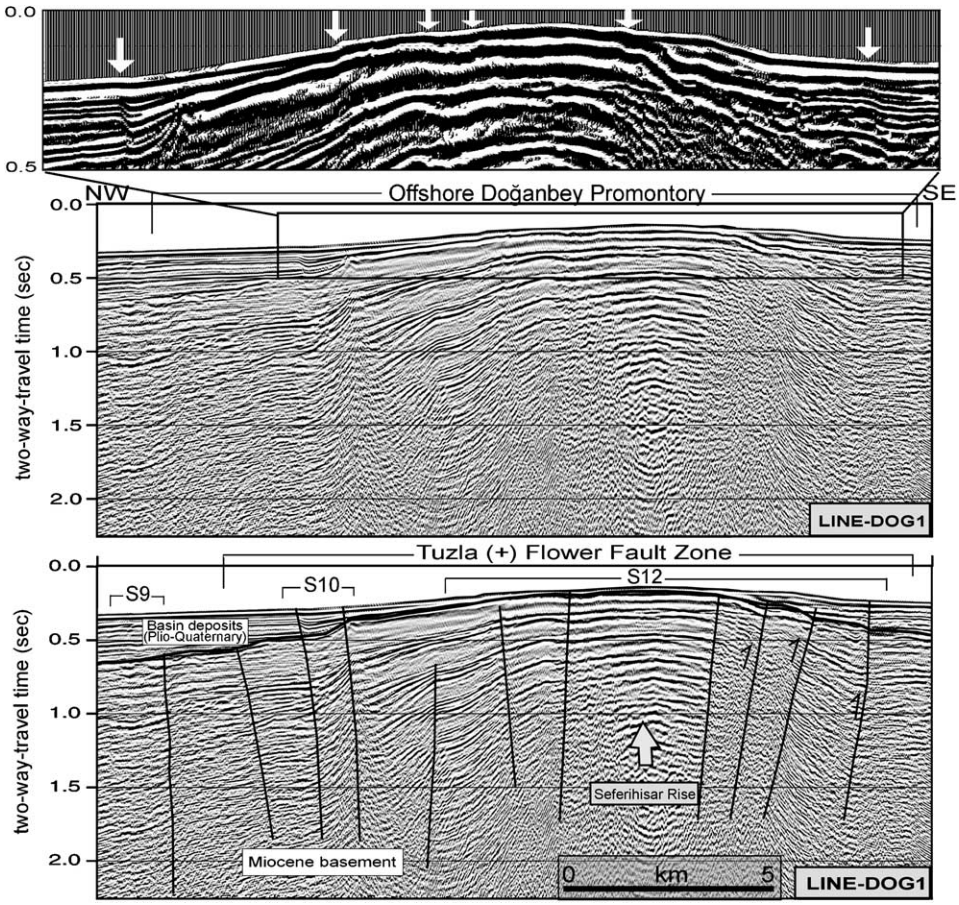

Fig. 10. Part of line Dog-1 located offshore of Doğanbey promontory. This seismic section shows a basement high and a large active positive flower structure with a reverse component at its southeast. This fault is associated with a right-lateral strike-slip fault which is called the Tuzla Fault (TF) onland. The white arrows in zoomed section on top show the active faults. Vertical exaggeration is ~ 2.5.

(TF). Strike-slip faults transform to reverse faults where their orientations change from NW–SE or NE–SW direction to N–S direction, such as Karaburun fault (KF). A simplified fault map (Fig. 11B) shows that the fault pattern of the study area can be explained by the pure-shear model (Fig. 11C). E–W compression in the area causes N–S trending reverse faults, E–W oriented normal faults, NE–SW oriented right lateral faults and NW–SE oriented left-lateral faults which correspond to Karaburun Fault, İzmir Fault, Tuzla Fault and NW–SE oriented strike-slip faults, respectively. Based on this interpretation, İzmir Gulf and the surrounding area shorten in E–W direction thus some uplifting occurs on Karaburun Peninsula and Seferihisar ridge along Karaburun and Tuzla faults (correlate Fig. 11B with Fig. 11C). GPS strain rates also support this pure-shear model in the study area with N–S extension and E–W compression strain vectors (Fig. 1). This tectonic framework shows that the structures in the study area are not compatible with adjacent areas. The fault patterns indicate that E–W trending grabens of western Anatolia such as Gediz and Küçük Menderes do not continue towards to west. On the contrary, they are delimited westward by N–S to NE–SW trending strike-slip faults of the study area. We interpret that the Tuzla Fault Zone has not only local but

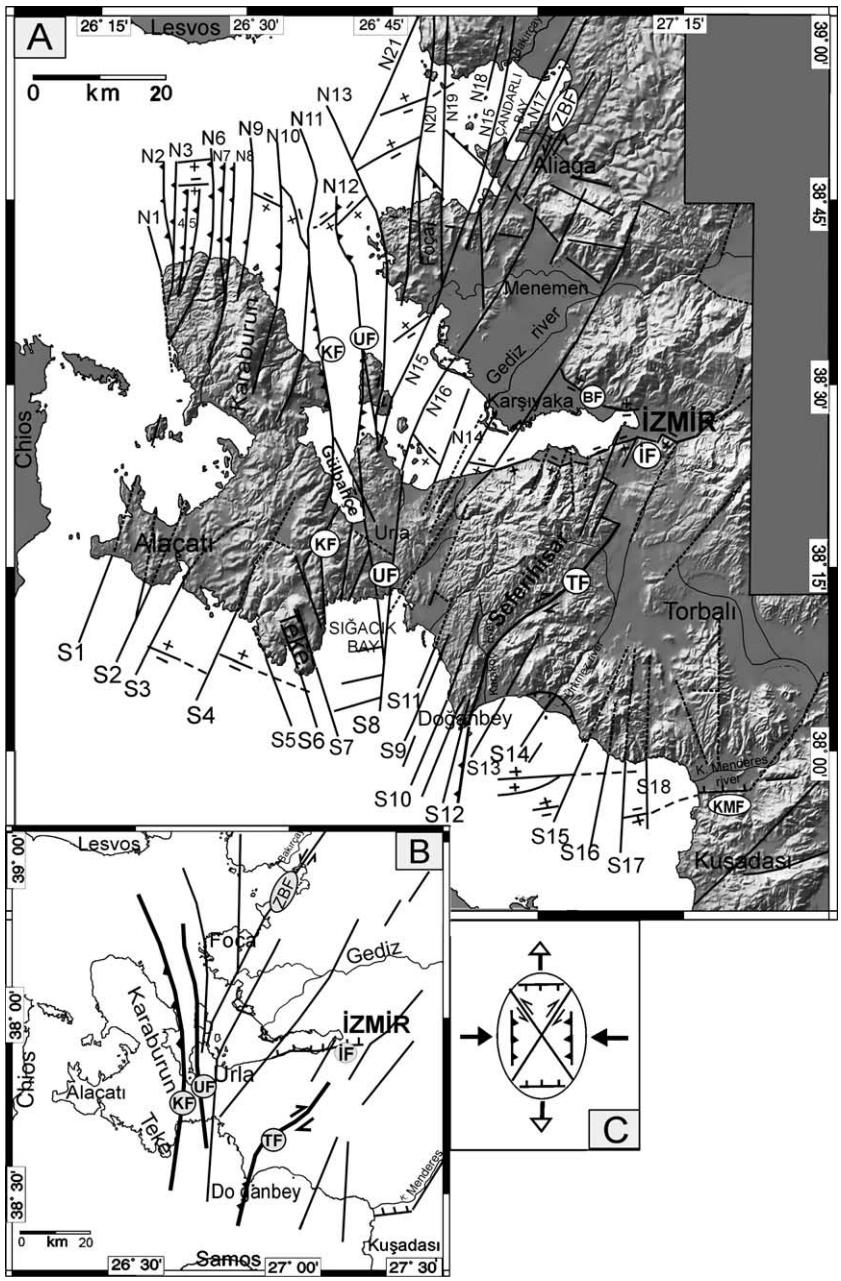

Fig. 11. (A) The correlations between offshore and onshore active fault systems in the study region. N–S, NE–SW and NW–SE oriented lines and dashed-lines show interpreted active strike-slip faults and their possible extensions. These faults are annotated with 'N' for those at north and 'S' for those at south. E–W oriented lines and dashed lines show interpreted active normal faults and their possible continuations, with footwalls indicated by the plus symbol. (B) Simplified active fault map of the study area. The bold lines show the master active faults. (C) Pure-shear model can explain the development of active structures in the study area.

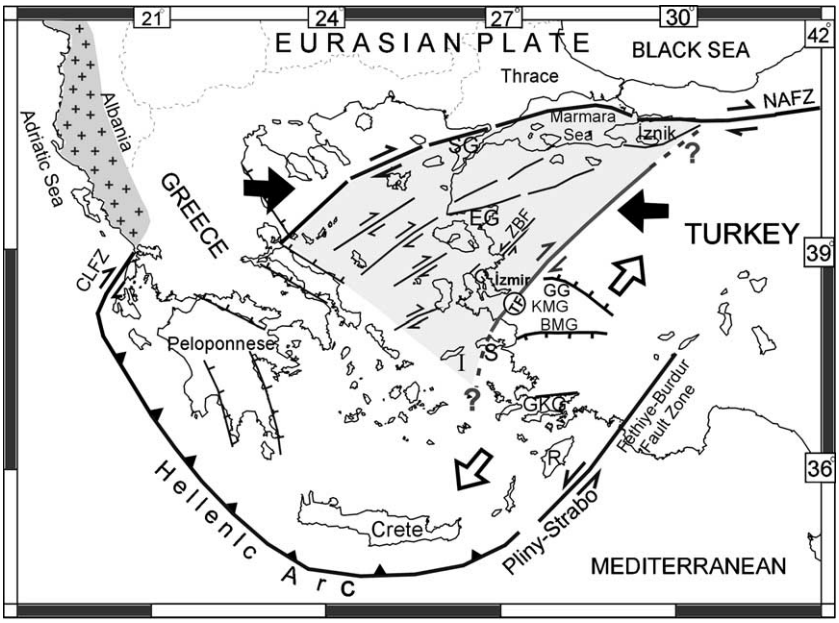

Fig. 12. Proposed cartoon model. The Tuzla strike-slip fault zone (TFZ) and its probable continuation towards the İznik at the north and towards the Samos island at the south constitutes the eastern border of the northern Aegean area (gray area). This transition zone separates the western Anatolian grabens such as Gediz (GG), Küçük Menderes (KMG), Büyük Menderes grabens (BMG) from the NE–SW trending structures of northern Aegean area. In the south of this transition zone, there is a rapid extension toward the Hellenic Trench. Abbrevations are: NAFZ—North Anatolian Fault Zone, SG—Saros Gulf, EG—Edremit Gulf, ZBF—Zeytindağ-Bergama Fault, İG—İzmir Gulf, S—Samos island, I—Ikaria island, GKG—Gökova Graben, R—Rodos island, CLFZ—Cephalonia–Lefkada Fault Zone.

also regional importance, as illustrated in a cartoon model (Fig. 12). The Tuzla Fault Zone probably extends towards İznik at the north. The presence of a zone of seismicity (Fig. 1) also supports the presence of this transition zone which separates the northern Aegean from the southern Aegean. Changes of GPS strain rates (Fig. 1) also support such a transition zone in the area (Fig. 12). We propose that the northern part (gray area on Fig. 12) of this transition zone is under E–W compression and N–S extension regime probably due to resistance of mainland Greece against the westward motion of Northern Anatolia (Fig. 12). The compression in this area is shown by Yaltırak et al. (2000, 2002) and Güney et al. (2001) in Saros and Edremit Gulfs and in the western Marmara Sea. E–W shortening in the northern Aegean area probably causes NE–SW sliding in this region from north to south such as the right lateral strike-slipe branches of the NAFZ, the Zeytindağ Bergama Fault Zone (ZBF) (Şaroğlu et al., 1992) and the Tuzla Fault Zone (TFZ) (Emre and Barka, 2000; Tan and Taymaz, 2001) (Fig. 12). From this point of view, the northern Aegean area can also be interpreted as Marmara block behaving as a separate tectonic unit as proposed by Crampin and Evans (1986). On the other hand, the southwest Anatolia and Aegean Sea, which is though to be at the southern part of this transition zone rapidly moves towards the Hellenic trench by right lateral Tuzla Fault and left-lateral Pliny–Strabo fault zones. GPS strain rates in the southwest Anatolia and south Aegean Sea support the rapid extension in this area (Fig. 1, Kahle et al., 1998; McClusky et al., 2000).

Acknowledgements

This study is a part of the Turkish National Marine Geology and Geophysics Program (coordinator: Naci Görür) carried out under TÜBİTAK projects 198Y079 and 100Y084. We thank the captain and crew of the MTA Sismik-1 research vessel for their efforts during data acquisition. We also thank the Department of

Navigation, Hydrography and Oceanography of the Turkish Navy for providing bathymetric data. Fahri Esenli provided the topographic data, which was digitised and edited by Erkan Gökaşan, Cem Gazioğlu and Zeki Yaşar Yücel. Maps were produced by GMT software package (Wessel and Smith, 1995).

References

Altunkaynak, Ş., Yılmaz, Y., 2000. Geology and Active Tectonic of Foça Area, Western Anatolia. BAD SEM 2000 Symp., İzmir, pp. 160–165. Ext. abstract.

Barka, A., 1992. The north Anatolian fault zone. Ann. Tecton., 164–195 (Suppl. To VI).

Barka, A., Kadinsky-Cade, K., 1988. Strike-slip fault geometry in Turkey and its influence on earthquake activity. Tectonics 7, 663–684.

Barka, A., Reilinger, R., 1997. Active tectonics of the eastern Mediterranean region: deduced from GPS, neotectonic and seismicity data. Ann. Geofis. XL (3), 587–610.

Crampin, S., Evans, R., 1986. Neotectonics of the Marmara sea region of Turkey. J. Geol. Soc. (Lond.) 143, 343–348.

Dewey, J.F., Şengör, A.M.C., 1979. Aegean and surrounding regions. Complex multiplate and continuum tectonics in a convergent zone. Geol. Soc. Amer. Bull. 90, 84–92.

Drakopoulos, J., Delibasis, N., 1982. The focal mechanism of earthquakes in the major area of Greece for the period 1947–1981. Seismol. Lab. Univ. Athens Publ. 2, 1–72.

Dumont, J.F., Uysal, Ş., Şimşek, S., Karamanderesi, H., Letouzey, J., 1979. Formation of the grabens in southwestern Anatolia. Bull. Miner. Res. Explor. Ins. Turk. 92, 7–18.

Emre, Ö., Barka, A., 2000. Active Faults Between Gediz Graben and Aegean Sea (İzmir Region). BAD SEM 2000 Symp., İzmir. Abstract.

Erinç, S., 1955. Die morphologischen Entwicklungsstadien der Küçük Menderes-masse. Rev. Univ. İstanbul Geogr. Inst. 2, 93–95.

Genç, C., Altunkaynak, Ş., Karacık, Z., Yazman, M., Yılmaz, Y., 2001. The Çubukludağ graben, south of İzmir: tectonic significance in the Neogene geological evolution of the Western Anatolia. Geodin. Acta 14, 1–12.

Güney, B.A., Yılmaz, Y., Demirbağ, E., Ecevitoğlu, B., Arzuman, S., Kuşçu, İ., 2001. Reflection seismic study across the continental shelf of Baba Burnu promontory of Biga Peninsula, Northwest Turkey. Mar. Geol. 176, 75–85.

Huguen, C., Mascle, J., Chaumillon, E., Woodside, J.M., Benkhelil, J., Kopf, A., Volkonskaia, A., 2001. Deformational styles of the eastern Mediterranean ridge and surroundings from combined swath mapping and seismic reflection profiling. Tectonophysics 343, 21–27.

Kahle, H.-G., Straub, C., Reilinger, R., McClusky, S., King, R., Hurst, K., Veis, G., Kastens, K., Cross, P., 1998. The strain rate field in the eastern Mediterranean region, estimated by repeated GPS measurements. Tectonophysics 294, 237–252.

Kalafat, D., 1995. Anadolu'nun tektonik yapılarının deprem mekanizmaları açısından irdelenmesi. Doctora thesis. İstanbul Universitesi, İstanbul.

Kaya, O., 1979. Ortadoğu Ege çöküntüsünün (Neojen) stratigrafisi ve tektoniği. Türk. Jeol. Kurult. Bül. 22, 35–58.

Kaya, O., 1981. Miocene reference section for the coastal parts of west Anatolia. Newsl. Stratigr. 10 (3), 164–191.

Kocaefe, S., Ataman, G., 1976. Actual tectonics of the western Anatolia. Yerbilimleri 9, 149–162.

Kurt, H., Demirbağ, E., Kuşçu, İ., 1999. Investigation of the submarine active tectonism in the Gulf of Gökova, southwest Anatolia–southeast Aegean Sea, by multi-channel seismic reflection data. Tectonophysics 305, 477–496.

Le Pichon, X., Angelier, J., 1979. The Hellenic Arc and trench system: a key to the tectonic evolution of the eastern Mediterranean area. Tectonophysics 60, 1–42.

Lykousis, V., Anagnostou, C., Pavlakis, P., Rousakis, G., Alexandi, M., 1995. Quaternary sedimentary history and neotectonic evolution of the eastern part of Central Aegean Sea, Greece. Mar. Geol. 128, 59–71.

Mascle, J., Martin, L., 1990. Shallow structure and recent evolution of the Aegean Sea: a synthesis based on continuous reflection profiles. Mar. Geol. 94, 271–299.

McKenzie, D.P., 1972. Active tectonics of Mediterranean region. Geophys. J. R. Astron. Soc. 30, 109–185.

McClusky, S., Balassanian, S., Barka, A., et al., 2000. Global Positioning system constraints on plate kinematics and dynamics in the eastern Mediterranean and Caucasus. J. Geophys. Res. 105, 5695–5719.

Piper, D.J.W., Perissoratis, C., 2003. Quaternary neotectonics of the South Aegean arc. Mar. Geol. 198, 259–288.

Seyitoğlu, G., Scott, B.C., 1994. Late Cenozoic basin development in west Turkey: Gördes basin: tectonics and sedimentation. Geol. Mag. 131, 631–637.

Stiros, S.C., Laborel, J., Deguen-Laborel, F., Papageorgiou, S., Evin, J., Pirazzoli, P.A., 2000. Seismic coastal uplift in a region of subsidence: Holocene raised shorelines of Samos Island, Aegean Sea, Greece. Mar. Geol. 170, 41–58.

Şaroğlu, F., Emre, Ö., Kuşçu, İ., 1992. Active fault map of Turkey, scale 1:2,000,000,000 Mineral Research and Exploration Institute of Turkey.

Şengör, A.M.C., Satır, M., Akkök, R., 1984. Timing of tectonic events in the Menderes Massif, western Turkey: implications for tectonic evolution and evidence for Pan-African basement in Turkey. Tectonics 3, 693–707.

Şengör, A.M.C, Görür, N., Şaroğlu, F., 1985. Strike-slip faulting and basin formation in zones of tectonic escape: Turkey as a case study. In: Biddle, K.T., Christie-Blick, N. (Eds.), Strike-slip Faulting and Basin Formation, Soc. Econ. Paleontol. And Mineral., Spec. Publ., vol. 37, pp. 227–264.

Tan, O., Taymaz, T., 2001. Source parameters of November 6, 1992 Doğanbey (Izmir) earthquake (M_w=6.0) obtained from inversion of teleseismic body-waveforms. 4th International Turkish Geology Symposium 24–28 September, 2001, Çukurova University, Adana, Turkey. Abstract volume, p.171.

Tan, O., Taymaz, T., 2003. Seismotectonics of Karaburun Peninsula and Kuşadası Gulf: Source Parameters of April 2, 1996 Kuşadası

Gulf and April 10, 2003 Seferihisar (İzmir) Earthquakes. International Workshop on the North Anatolian, East Anatolian and Dead Sea Fault Systems: Recent Progress in Tectonics and Paleoseismology and Field Training Course in Paleoseismology, Middle East Technical University (METU) 31 August–12 September 2003, Ankara, Turkey. Abstract volume, p.147.

Taymaz, T., Jackson, J.A., Mckenzie, D., 1991. Active Tectonics of the north and Central Aegean Sea. Geophys. J. Int. 106, 433–490.

Wessel, P., Smith, W.H.F., 1995. New version of the Generic Mapping Tools released. Eos 76 (33), 329.

Woodside, J., Mascle, J., Huguen, C., Volkonskaia, A., 2000. The Rhodes Basin, a post-Miocene tectonic trough. Mar. Geol. 165, 1–12.

Yaltırak, C., Alpar, B., Sakınç, M., Yüce, H., 2000. Origin of the Strait of Çanakkale (Dardanelles): regional tectonics and the Mediterranean–Marmara incursion. Mar. Geol. 164, 139–159.

Yaltırak, C., Sakınç, M., Aksu, A.E., Hiscott, R.N., Galleb, B., Ulgen, U.B., 2002. Late Pleistocene uplift history along the southwestern Marmara Sea determined from raised coastal deposits and global sea-level variations. Mar. Geol. 190 (1-2), 283–305.

Yılmaz, Y., Genç, Ş.C., Gürer, F., Bozcu, M., Yılmaz, K., Karacık, Z., Altunkaynak, Ş., Elmas, A., 2000. When did the western Anatolian grabens begin to develop? In: Bozkurt, E., Winchester, J.A., Piper, J.D.A. (Eds.), Tectonics and Magmatism in Turkey and Surrounding Area, Geol. Soc. London Spec. Publ., vol. 173, pp. 353–384.